Dynamic Uncertainty-Aware Dispatch for Flexible Ramping Products with Guaranteed Deliverability

Omar Abu-Znad, Mingyu Zhai, and Liang Du
Department of Electrical & Computer Engineering
Villanova University
Villanova , USA
{oabuznad, mzhai, liang.du}@villanova.edu

Fengyu Wang
School of Electrical & Computer Engineering
New Mexico State University
Las Cruces, New Mexico, USA
fywang@nmsu.edu

***Abstract*—Flexible ramping products have been widely adopted to improve grid flexibility and reliability. However, existing practices often lead to undeliverable ramping awards that are frequently assigned to generators constrained by the transmission network, along with inflated reserve requirements arising from proxy-based uncertainty estimation. This paper proposes a flexible ramping dispatch framework that integrates data-driven, multi-time-scale dynamic uncertainty and locational flexibility. The proposed approach guarantees ramping capacities remain feasible under transmission constraints while reducing ramping requirements through intra-hour-aware uncertainty modeling. The model is validated on a modified IEEE 118-bus system using real-world data and benchmarked against existing system-wide and zonal flexible ramping designs. Results demonstrate that incorporating locational flexibility improves allocation efficiency, ensures deliverability, and enhances system reliability.**

***Index Terms*—Locational Flexibility, Flexible Ramping Products, Deliverability, Dynamic Uncertainty.**

I. Introduction

The growing integration of renewable energy resources has intensified the net-load variability and uncertainty in modern power systems, posing significant challenges to maintain the balance between generation and net-demand. Ramping capacity shortages introduce a critical challenge to reliable system operation and emphasize the need to enhance grid flexibility. Various approaches have been explored to enhance operational flexibility, such as the integration of Fast-Start (FS) units and Energy Storage Systems (ESSs). Despite these efforts, such solutions entail high costs, motivating Independent System Operators (ISOs) to enhance existing market mechanisms by incorporating variability and uncertainty into market models. Recently, several ISOs have implemented Flexible Ramping Products (FRPs) to mitigate ramp scarcity issues [1]–[3]. However, post-implementation evaluations of these products revealed that FRPs had limited impact in reducing the expensive out-of-market solutions, with California ISO (CAISO) even reporting increased manual interventions [4]. This issue often arises from FRPs being frequently awarded to generators located behind transmission constraints, leading to stranded products, and low FRP prices, even in the cases with limited ramping capability in the system.

Recently, CAISO highlighted the deliverability issue and proposed nodal procurement of FRPs as a potential solution [5]. In [6], the authors introduced nodal and zonal models to support this approach. Although these models enable nodal procurement, they fall short of explicitly accounting for nodal flexibility. Incorporating locational flexibility ahead of dispatch can further strengthen this framework by revealing potential binding constraints and enhancing ISO decision-making. The literature has thoroughly examined flexibility quantification and characterization on the distribution side [7], [8], while studies on flexibility on the transmission side remain relatively scarce. Existing works primarily characterize system flexibility through region-based formulations in generation or demand spaces [9], [10]. However, existing studies often overlook the post-deployment deliverability of flexibility, which can result in stranded ramping reserves. Post-deployment deliverability has been examined in [4] and [11], where the former proposed a two-pass market framework to improve FRP procurement, while the latter developed a distributionally robust, chance-constrained multi-interval OPF model considering spatio-temporal uncertainty. Although both achieved promising results, their reliance on robust and stochastic formulations contrasts with the original intent of these ramping reserves to preserve existing market structures while addressing variability and uncertainty, highlighting the need for models consistent with current market practices. An additional issue in the current flexible ramping design is the proxy-based requirement quantification. Recent ISO practices and prior academic studies [4], [12] typically determine ramping requirements using proxy-based system-wide or zonal values derived from a fixed percentile of forecast uncertainty. While proxy-based requirements capture a portion of uncertainty, they neglect its dynamic evolution and often overestimate ramping needs, leading to inflated system costs. In response, Midcontinent Independent System Operator (MISO) has highlighted this issue and is exploring dynamic ramp capability frameworks to better represent time-varying uncertainty in ramping requirement formulation [13].

To address these limitations, this paper proposes a deliverability-aware flexible ramping dispatch framework that integrates data-driven, multi–time-scale dynamic uncertainty with locational flexibility, enabling efficient and accurate ramp allocation with guaranteed deliverability and improved reliability. Table I shows that existing works often lack one or more features essential for effective deployment.

979-8-3315-8138-1

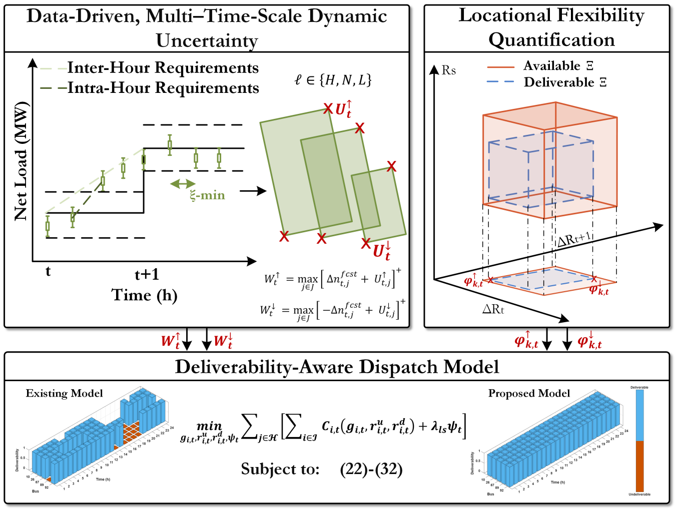

Fig. 1. Overview of the proposed framework.

TABLE I
SUMMARY OF KEY STUDIES.

Ref.	Market Consistency	Dynamic Uncertainty	Deliverability	Intra-hour Variability
[4]	✗	✗	✓	✓
[6]	✓	✗	Partial	✓
[9]	✗	✗	Partial	✗
[11]	✗	✓	✓	✗
[12]	✓	✗	✗	✓
Proposed	✓	✓	✓	✓

II. PROBLEM FORMULATION

In this study, the scheduling horizon is set to one day. Let $\mathcal{H} = \{1, \dots, T\}$ denote the set of hourly time periods, each divided into fixed intra-hour intervals of ξ minutes (e.g., $\xi = 5, 10, 15$). Define the intra-hour index set as $\mathcal{J} = \{0, \xi, 2\xi, \dots, 60 - \xi\}$. The power system comprises a set of buses $\mathcal{K} = \{1, \dots, N_k\}$, generators $\mathcal{I} = \{1, \dots, N_i\}$, and transmission lines $\mathcal{L} = \{1, \dots, N_l\}$. For zonal analysis, the network is partitioned into zones $\mathcal{Z} = \{1, \dots, Z\}$. For each $t \in \mathcal{H}$ and $j \in \mathcal{J}$, the variable $x_{t,j}$ represents the value of x at minute j within hour t. The following subsections present the proposed framework that integrates dynamic flexible ramping design with locational flexibility awareness into a deliverability-aware dispatch model. The framework is illustrated in Fig. 1.

A. Flexible Ramping Requirements

The traditional approach computes ramping requirements as the sum of net-load variability and uncertainty. Let n_t^{fcst} denotes the forecast system net-load (MW) for hour t. The hourly upward and downward ramping requirements are given by:

$$W_t^{\uparrow} = \left[\Delta n_t^{\text{fcst}} + \hat{up}_{t+1}\right]^+, \qquad \forall t, \tag{1}$$

$$W_t^{\downarrow} = \left[-\Delta n_t^{\text{fcst}} + \hat{dn}_{t+1}\right]^+, \qquad \forall t, \tag{2}$$

where $\Delta n_t^{\text{fcst}} = (n_{t+1}^{\text{fcst}} - n_t^{\text{fcst}})$, and $\hat{up}_{t+1}$ and $\hat{dn}_{t+1}$ are the upward and downward uncertainty (MW), and $[x]^+ = \max\{x, 0\}$. However, this approach overlooks essential system characteristics. It handles uncertainty through a fixed percentile, neglecting its temporal evolution and spatial correlation across system zones, and it fails to capture the sub-hour ramp variability that can affect real-time feasibility. In this work, a data-driven zonal ramping requirement framework that incorporates dynamic uncertainty and intra-hour variability is proposed to address these shortcomings.

It is essential to account for the sub-hour steep ramping to ensure feasibility in real-time operations. Let $n_{t,j}^{\text{fcst}}$ and $n_{t,j}^{\text{act}}$ be the forecast and actual net-load, respectively, and $n_{t,j}^{(\cdot)} = \sum_{z \in \mathcal{Z}} n_{z,t,j}^{(\cdot)}$. The intra-hour-aware variability is defined as:

$$\Delta n_{t,j}^{\text{fcst}} := n_{t,j+\xi}^{\text{fcst}} - n_{t,j}^{\text{fcst}}, \tag{3}$$

$$\Delta n_{t,j}^{\text{act}} := n_{t,j+\xi}^{\text{act}} - n_{t,j}^{\text{act}}, \tag{4}$$

and the ramp forecast error is defined as:

$$\varepsilon_{z,t,j} := \Delta n_{z,t,j}^{\text{act}} - \Delta n_{z,t,j}^{\text{fcst}}, \tag{5}$$

the corresponding upward and downward ramp forecast error terms are $\varepsilon_{z,t,j}^+ := \max(\varepsilon_{z,t,j}, 0)$ and $\varepsilon_{z,t,j}^- := \max(-\varepsilon_{z,t,j}, 0)$.

This work utilizes real-world historical data to define upper bounds for the upward and downward ramping errors denoted by $u_{z,j}^{(\ell)}$ and $d_{z,j}^{(\ell)}$, respectively. The superscript ℓ indicates the system condition level, categorized as high, normal, or low such that $\ell \in \{H, N, L\}$. System operating conditions are classified into high (H), normal (N), and low (L) uncertainty levels based on historical net-load ramp forecast errors and intra-hour variability. Periods with larger forecast errors and steeper ramps are treated as high-uncertainty conditions, while more stable periods are classified as low-uncertainty. This data-driven classification allows the uncertainty sets to adapt dynamically using indicators readily available to system operators.

The resulting polyhedral sets of admissible zonal errors are:

$$\mathcal{U}_{t,j}^{\uparrow}(\ell) = \left\{ \varepsilon^+ \in \mathbb{R}_+^Z \;\middle|\; \begin{array}{ll} 0 \le \varepsilon_{z,t,j}^+ \le u_{z,j}^{(\ell)} & \forall z, \\ \displaystyle\sum_{z=1}^{Z} \frac{\varepsilon_{z,t,j}^+}{u_{z,j}^{(\ell)}} \le \Gamma_{j,\uparrow}^{(\ell)} & \end{array} \right\}, \tag{6}$$

$$\mathcal{U}_{t,j}^{\downarrow}(\ell) = \left\{ \varepsilon^- \in \mathbb{R}_+^Z \;\middle|\; \begin{array}{ll} 0 \le \varepsilon_{z,t,j}^- \le d_{z,j}^{(\ell)} & \forall z, \\ \displaystyle\sum_{z=1}^{Z} \frac{\varepsilon_{z,t,j}^-}{d_{z,j}^{(\ell)}} \le \Gamma_{j,\downarrow}^{(\ell)} & \end{array} \right\}, \tag{7}$$

where $\Gamma_{j,\uparrow}^{(\ell)}$ and $\Gamma_{j,\downarrow}^{(\ell)}$ are the spatial correlation budgets which are calibrated based on the correlation matrix. Therefore, equations (1) and (2) are reformulated as:

$$W_t^{\uparrow} = J \times \big(\max_{j \in \mathcal{J}} \left[\Delta n_{t,j}^{\text{fcst}} + U_{t,j}^{\uparrow}\right]^+\big), \tag{8}$$

$$W_t^{\downarrow} = -J \times \big(\max_{j \in \mathcal{J}} \left[-\Delta n_{t,j}^{\text{fcst}} + U_{t,j}^{\downarrow}\right]^+\big), \tag{9}$$

where $U_{t,j}^{\uparrow}$ / $U_{t,j}^{\downarrow}$ are worst-case errors in the uncertainty sets.

979-8-3315-8138-1

B. Locational Flexibility Quantification

Accurately assessing locational flexibility is essential to ensure ramp deliverability and avoid awarding reserves to generators behind transmission constraints. Unlike [6], which focuses on bus-level ramping requirements, locational flexibility provides deeper insight into which network constraints are likely to bind and when it maybe violated [10]. Accordingly, this work proposes a locational flexibility quantification model.

The flexibility region is defined by linear constraints on the system state variables, forming a polytope in H-representation.

$$\Xi = \{X \mid AX \leq b\}, \tag{10}$$

where X is the variable vector, A and b represent the system parameters. The variable vector can represent the system power, ramping, or energy. The available system-wide flexibility is defined, then, the locational flexibility is introduced.

The bounds of possible ramping deviations at each bus are defined as:

$$\tilde{r}_{k,t} + \Delta r_{k,t} = \frac{1}{\Delta t}\left(p_{k,t+1} - p_{k,t}\right), \quad \forall t \tag{11}$$

where $\tilde{r}_{k,t}$ is the scheduled ramping of the bus and $\Delta r_{k,t}$ is the possible deviation. The system-wide ramping deviations:

$$R_s + R_d = P, \tag{12}$$

where $R_s = \sum_{k=1}^{N_k} \tilde{r}_{k,t}$ denotes the total scheduled ramping capacity, $R_d = \sum_{k=1}^{N_k} \Delta r_{k,t}$ represents the aggregate ramping deviation, and $P = (P_{t+1} - P_t)/\Delta t$ is the system-wide net-load ramping requirement.

The system-wide ramping flexibility is defined as:

$$\Xi_s = \left\{R \in \mathbb{R}^{N_s+N_d} \,\middle|\, [A \quad B]\, R \leq b\right\}, \tag{13}$$

where $R = [R_s^\top, R_d^\top]^\top$, and N_s/N_d are the number of sources providing the flexibility and the number of deviations, respectively. The operational characteristics of the generation units i in each bus are defined as:

$$\underline{g}_i \leq g_{i,t} \leq \overline{g}_i, \quad \forall t \tag{14}$$

$$-\underline{\delta}_i \Delta t \leq g_{i,t+1} - g_{i,t} \leq \overline{\delta}_i \Delta t, \quad \forall t \tag{15}$$

where $g_{i,t}$ is the generator output, $\underline{g}_i$ and $\overline{g}_i$ are its limits, and $\underline{\delta}_i$, $\overline{\delta}_i$ are ramp limits.

To ensure deliverable locational ramping capacity at each bus, the following transmission constraints are included.

$$\sum\nolimits_{i\in\mathcal{I}_k} \left(\tilde{g}_{i,t} + \Delta g_{i,t}\right) - d_{k,t} = 0, \quad \forall k, t \tag{16}$$

$$-f_l^{\max} \leq \sum\nolimits_{k=1}^{N_k} \Phi_{l,k}\big(\tilde{g}_{k,t} + \Delta g_{k,t} - d_{k,t}\big) \leq f_l^{\max}, \quad \forall l, t \tag{17}$$

constraint (16) ensures the balance between demand and generation, and constraint (17) is the maximum transmission line load, Φ is the sensitivity of bus injections into flows and $f_l^{\max}$ is the line capacity.

Locational flexibility is defined as the projection of the system-wide flexibility region onto the subspace of net-load deviations at a selected bus k, characterizing the set of deviations that can be feasibly balanced at that bus. Formally, it is defined as:

$$(13) \underset{\text{Project}}{\Rightarrow} \Xi_k = \left\{ R_k \in \mathbb{R} \,\middle|\, \exists R \in \Xi_s \,, R_k = \Pi_k R\right\}, \tag{18}$$

where Π_k projects the system-wide feasible space Ξ_s onto the subspace of bus k, representing all network-feasible ramping realizations at that location. The deliverability bounds are:

$$\varphi_{k,t}^{\uparrow} = \max_{R_k \in \Xi_k} \left[R_{k,t}\right]^+, \quad \forall k, t \tag{19}$$

$$\varphi_{k,t}^{\downarrow} = \max_{R_k \in \Xi_k} \left[-R_{k,t}\right]^+. \quad \forall k, t \tag{20}$$

The projection step reduces to solving linear programs that are independent across buses and time intervals, enabling parallel computation or restriction to potentially binding locations and resulting in a modest, scalable computational burden.

C. Deliverability Guarantees

The bounds $\varphi_{k,t}^{\uparrow}$ and $\varphi_{k,t}^{\downarrow}$ obtained in (19)–(20) represent the extreme deliverable ramping deviations at bus k, derived directly from the locational flexibility region Ξ_k in (18) as illustrated in Fig. 1. Since the region Ξ_k is constructed from the projection of the system-wide flexibility region Ξ_s while explicitly enforcing the network power-balance and transmission constraints, each point within Ξ_k corresponds to a physically feasible and network-consistent operating condition. Consequently, any feasible ramping allocation $r_{k,t} \in [\varphi_{k,t}^{\downarrow}, \varphi_{k,t}^{\uparrow}]$ is guaranteed to be deliverable within the network limits. This ensures that the awarded ramping products are not stranded behind transmission constraints and that all dispatched capacities remain physically realizable in real-time operations. Therefore, the deliverability guarantees are inherently embedded within the proposed flexibility formulation through the construction of Ξ_k and its derived bounds $(\varphi_{k,t}^{\uparrow}, \varphi_{k,t}^{\downarrow})$.

D. Deliverability-Aware Dispatch Model

In this paper, energy and flexible ramping products $g_{i,t}$, $r_{i,t}^u$, and $r_{i,t}^d$ are co-optimized to ensure deliverability and efficient ramp allocation. The proposed multi-period dispatch model minimizes the total generation cost and load shedding ψ_t.

$$\min_{g_{i,t}, r_{i,t}^u, r_{i,t}^d, \psi_t} \ \sum\nolimits_{t\in\mathcal{H}} \left[\sum\nolimits_{i\in\mathcal{I}} C_{i,t}\big(g_{i,t}, r_{i,t}^u, r_{i,t}^d\big) \ + \ \lambda_{ls}\, \psi_t\right], \tag{21}$$

subject to:

$$g_{i,t} + r_{i,t}^u \leq \overline{g}_i, \quad \forall i, t \tag{22}$$

$$g_{i,t} - r_{i,t}^d \geq \underline{g}_i, \quad \forall i, t \tag{23}$$

$$r_{k,t}^u = \sum\nolimits_{i\in\mathcal{I}_k} r_{i,t}^u, \quad \forall k, t \tag{24}$$

$$r_{k,t}^d = \sum\nolimits_{i\in\mathcal{I}_k} r_{i,t}^d, \quad \forall k, t \tag{25}$$

$$\sum\nolimits_{k\in K} r_{k,t}^u \geq W_t^{\uparrow}, \quad \forall t \tag{26}$$

$$\sum\nolimits_{k\in K} r_{k,t}^d \geq W_t^{\downarrow}, \quad \forall t \tag{27}$$

$$0 \leq r_{k,t}^u \leq \varphi_{k,t}^{\uparrow}, \quad \forall k, t \tag{28}$$

$$0 \leq r^{d}_{k,t} \leq \varphi^{\downarrow}_{k,t}, \quad \forall k, t \tag{29}$$

$$\sum_{i \in \mathcal{I}} g_{i,t} + \psi_t = d_t, \qquad \forall t \tag{30}$$

$$-f_l^{\max} \leq \sum_{k=1}^{N_k} \Phi_{l,k}\big(g_{k,t} - d_{k,t}\big) \leq f_l^{\max}, \quad \forall l, t \tag{31}$$

$$(r^{u}_{i,t}, r^{d}_{i,t}) \in [0, \bar{\delta}_i] \times [0, \underline{\delta}_i], \tag{32}$$

where $C_{i,t}$ is convex and piecewise linear cost function, $r^{u}_{i,t}$ and $r^{d}_{i,t}$ are the upward ramping product and downward product, respectively. Constraints (22) and (23) are the generation limits, (24)-(27) ensures the ramping products for all buses satisfies the dynamic-uncertainty aware ramping requirements, and constraints (28) and (29) ensures the awarded ramping products for each bus are deliverable. Constraints (30) and (31) are the power balance and transmission network constraints, while (32) ensures the dispatched ramping limits are within the generation ramping capability.

III. Case Study

A. Test System Description

A modified IEEE 118-bus system with 54 generation units, 186 lines and 91 loads is used as a case study in this work [14]. The system has high renewable penetration that is distributed over three zones $\mathcal{Z} = \{1, 2, 3\}$. The Fifteen-Minute Market (FMM) operated by CAISO is considered the real-time market in this work, with $\xi = 15$. The hourly and 15-minute net-load and the solar and wind data used in this work are normalized real-world data from CAISO [15]. Data-driven polyhedral uncertainty sets are derived from historical 15-minute net-load forecast errors (96 time steps per day), capturing both inter-hour and intra-hour variability. The multi-time-scale uncertainties are modeled through zonal polyhedral sets constructed from historical ramp forecast errors. For each system condition $\ell \in \{H, N, L\}$, the polytope bounds are calibrated to empirical percentiles (97.5%, 87.5%, and 77.5%), resulting in dynamic, multi–time-scale ramp requirements used in the proposed dispatch model. The percentile levels are calibrated from historical intra-hour net-load ramp forecast errors using empirical quantiles. The 97.5^{th} percentile is selected for high-uncertainty periods as it provides effective coverage of extreme yet credible ramp realizations, while the 87.5^{th} and 77.5^{th} percentiles are used for normal and low-uncertainty conditions to reduce conservatism. The spatial budget parameters are calibrated from empirical correlation matrices of zonal forecast errors. The penalty for load loss λ_{ls} is considered \$10,000/MWh, which is a typical high value to penalize load loss and make it last resort [12]. GUROBI solver is used to solve the proposed convex optimization problem of the DA dispatch model on a computer with Intel(R) Core(TM) i9-14900HX 2.20 GHz and 32.0 GB RAM.

B. Deliverable Flexibility Visualization and Analysis

The locational ramping flexibility is quantified using Eq. (18). This ensures that the FRPs awarded for the selected bus are deliverable. The available ramp capacity in each bus is not always equal to the deliverable ramp capacity. A bus could

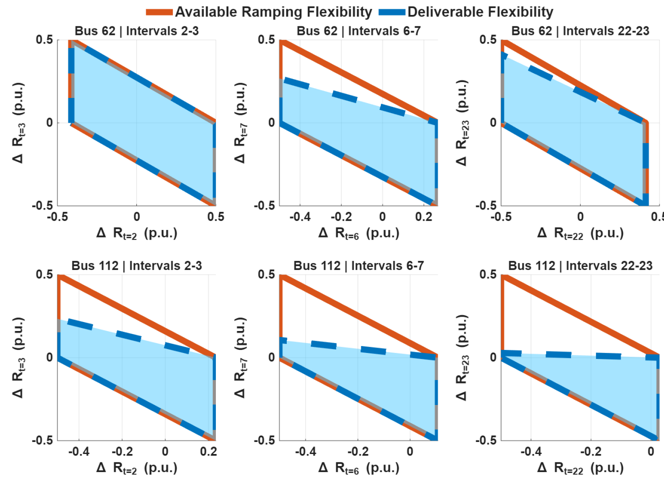

Fig. 2. Available and deliverable locational ramping flexibility at buses 62 and 112.

be located behind the transmission constraints, which means that its available ramping capacity cannot be fully delivered. Since the proposed model is multi-interval dispatch model, the deliverable flexibility is quantified and computed across all the intervals to optimize the control decision from the system operator. As shown in Fig. 2, each plot depicts the available and deliverable ramping flexibility at a selected bus over two consecutive time intervals. For example, the first plot illustrates bus 62 between time steps 2 and 3, where using upward ramping at time step 2 restricts ramping in the opposite direction at time step 3. For bus 62, the top three plots show that all available flexibility is fully deliverable at time steps 2-3, while partial undeliverability appears at time steps 6-7, and a slight reduction in deliverable flexibility is observed at time steps 22-23. The lower three plots illustrate the corresponding ramping flexibility behavior at bus 112. Buses 62 and 112 are selected to illustrate the impact of network location on deliverable flexibility: bus 62 is well connected with higher transmission capacity, while bus 112 is a peripheral bus with limited connectivity. Consequently, bus 62 exhibits greater deliverable ramping capacity. This insight allows the analysis to focus on potentially binding buses, reducing computational effort and demonstrating scalability.

C. Performance Evaluation of the Proposed Dispatch Model

The proposed multi-period day-ahead dispatch model is compared with system-wide (CAISO) and zonal (MISO) ramping designs under a fixed 97.5% uncertainty level to evaluate the benefits of incorporating locational flexibility and dynamic uncertainty. Fig. 3 shows the deliverability of upward ramping products for all generators over 24 hours, where the system-wide and zonal designs occasionally award undeliverable ramps, while the proposed model maintains full deliverability. The numerical results for the dispatch decisions over 24-hour period are listed in Table II. The effect of incorporating temporal coupling in net-demand uncertainties is reflected in the amount of dispatched flexible ramping reserves. The proposed model yields a significantly lower reserve dispatch as the uncertainty percentile is changed based

979-8-3315-8138-1

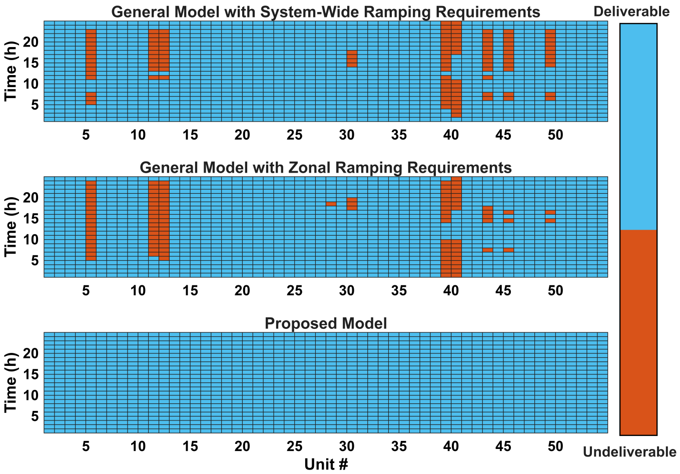

Fig. 3. Deliverability status of the upward ramping products over 24 hours.

on the system-level, thereby reducing the total system cost while still ensuring deliverability. The results highlight the importance of obtaining an optimal allocation of the flexible ramping product. When ramping capacity is not optimally allocated, as observed in the general model cases, reserves tend to be awarded to generators with low opportunity cost but limited deliverability, resulting in stranded products and increased real-time interventions. In contrast, the proposed model achieves an optimal allocation by explicitly accounting for network constraints and locational ramping capability, ensuring that the procured ramping reserves are both economically efficient and physically deliverable. This leads to reduced reserve over-procurement and improved system reliability. Although general model designs have a close number of time steps with inter-hour undeliverability, the system-wide design has significantly higher undeliverable products. The reason is that the zonal design better allocates the products among generators as it considers three distinct zones instead of the whole system. The benefit of accounting for intra-hour steep ramping requirements is reflected in the load-shedding results. The general model experiences load shedding because generators cannot satisfy intra-hour ramping needs despite meeting inter-hour requirements, leading to increased commitment of costly fast-start units and higher operating costs. Although re-dispatch in the 15-minute market improves intra-hour deliverability for the general model, instances of undeliverability persist under both designs. The sensitivity of the proposed framework to uncertainty confidence levels and spatial correlation budgets follows intuitive trends, with higher values increasing ramp procurement and cost and lower values reducing reserve requirements, while ramp deliverability remains preserved across all reasonable settings. The proposed model solves the day-ahead dispatch in approximately 2.3 seconds, comparable to the system-wide (2.0 s) and zonal (1.78 s) benchmarks, demonstrating computational tractability.

IV. Conclusion

This paper proposes a deliverability-aware flexible ramping dispatch framework that integrates dynamic uncertainty and locational flexibility under transmission constraints. By embedding deliverability bounds into the day-ahead dispatch, the model prevents stranded reserves and ensures physically feasible ramp allocations. Case studies on a modified IEEE 118-bus system using CAISO data demonstrate full ramp deliverability, elimination of scarcity hours and load shedding, and reduced ramp procurement compared to system-wide and zonal designs, with comparable computational performance. The proposed framework is compatible with existing ISO market designs through offline computation of locational deliverability bounds, while broader co-optimization with additional ancillary services is identified as a direction for future work.

TABLE II
Dispatch decisions over 24-hour period.

Dispatch Decisions	System	Zonal	Proposed
Dispatched FRPs [MWh]	53,833	53,838	48,874
Delivered FRPs [MWh]	46,102	48,808	48,874
Deliverability Ratio [%]	85.6	90.6	100
Scarcity Hours [#]	114	106	0
Load Shedding [MWh]	123.6	67.5	0
Scarcity Intervals in FMM [#]	43	31	0
CPU Time [s]	2	1.78	2.3

References

[1] California Independent System Operator (CAISO), "Day-ahead market enhancements," Tech. Rep., 2019.
[2] Midcontinent Independent System Operator (MISO), "Ramp product enhancements," 2022.
[3] Southwest Power Pool, "State of the market - Fall 2024," Tech. Rep.
[4] O. Yurdakul, E. Ela, and F. Billimoria, "Flexible ramping product procurement in day-ahead markets," *IEEE Transactions on Energy Markets, Policy and Regulation*, vol. 3, no. 1, pp. 13–31, 2025.
[5] CAISO, "Flexible ramping product performance," Tech. Rep., Mar 2022. [Online]. Available: https://www.caiso.com/documents/report-flexiblerampingproductperformance.pdf
[6] F. Wang and Y. Chen, "Market implications of short-term reserve deliverability enhancement," *IEEE Transactions on Power Systems*, vol. 36, no. 2, pp. 1504–1514, 2020.
[7] S. Wang, L. Du, B. Cui, and Y. Li, "Multi-factor-coupled, ahead-of-time aggregation of power flexibility under forecast uncertainty," *IEEE Transactions on Sustainable Energy*, vol. 16, no. 2, pp. 892–903, 2025.
[8] S. Wang, L. Du, and X. Chen, "Bayesian active learning-based soft data space calibration for system-wise aggregate flexibility characterization," *IEEE Transactions on Smart Grid*, 2025.
[9] H. Wang and Z. Bie, "Data-driven distributionally robust energy and reserve scheduling considering res flexibility," *IEEE Transactions on Power Systems*, vol. 40, no. 3, pp. 2438–2450, 2025.
[10] M. Awadalla and F. Bouffard, "Flexibility characterization of sustainable power systems in demand space: A data-driven inverse optimization approach," *IEEE Transactions on Power Systems*, vol. 39, no. 5, pp. 6196–6209, 2024.
[11] X. Fang, K. S. Sedzro, H. Yuan, H. Ye, and B.-M. Hodge, "Deliverable flexible ramping products considering spatiotemporal correlation of wind generation and demand uncertainties," *IEEE Transactions on Power Systems*, vol. 35, no. 4, pp. 2561–2574, 2020.
[12] M. Ghaljehei and M. Khorsand, "Day-ahead operational scheduling with enhanced flexible ramping product: Design and analysis," *IEEE Transactions on Power Systems*, vol. 37, no. 3, pp. 1842–1856, 2022.
[13] Midcontinent Independent System Operator (MISO), "Dynamic ramp capability product requirement (uncertainty component)," 2024.
[14] I. Peña, C. B. Martinez-Anido, and B.-M. Hodge, "An extended ieee 118-bus test system with high renewable penetration," *IEEE Transactions on Power Systems*, vol. 33, no. 1, pp. 281–289, 2018.
[15] CAISO, "California ISO Open Access Same-time Information System (OASIS)," http://oasis.caiso.com/, 2024.

979-8-3315-8138-1